*35th EPS Conference on Plasma Phys. Hersonissos, 9 - 13 June 2008 ECA Vol.**32D**, P-1.133 (2008)*

Phase-sensitive Terahertz Plasma Emission from Gas Targets Irradiated by Few-cycle Intense Laser Pulses

Hui-Chun Wu* and Jürgen Meyer-ter-Vehn

Max Planck Institute for Quantum optics, Garching, Germany

Abstract

When an electron in the atom is ionised in the intense laser field, it can obtain the net momentum in the laser polarization direction. After the passing of the laser pulse, these free electrons move in the plasma and radiate the electromagnetic pulse with the plasma frequency. When the plasma density is within 10^{16}-10^{18}cm^{-3}, the radiation is in the terahertz (THz) region. By analysis and two-dimensional particle-in-cell (2DPIC) simulation, we find that THz emission strength is sinusoidally dependent on the carrier-envelope-phase (CEP) of few-cycle laser pulses. This phenomenon can service as a potential approach to measure the CEP. We find the favourable parameters for this application [1].

1. Net momentum and radiation dipole

Once the electron is released from the atom, its motion is governed by the laser field. For a free electron in a plane wave, we have the constant of motion $\vec{p}_\perp(t) - e\vec{A}_\perp(t) = const.$ [2], where $\vec{p}_\perp(t)$ is the transverse momentum of electron, $\vec{A}_\perp(t)$ is the transverse vector potential of laser pulse, and -e is the electron charge. At the electron's birth time, one has $\vec{p}_\perp(t = t_b) = 0$. After the laser pulse has passed, the field is $\vec{A}_\perp(t = \infty) = 0$. Using the conservation of canonical momentum, one then obtains the final momentum of the electron

$$\vec{p}_\perp(t = \infty) = -e\vec{A}_\perp(t = t_b). \qquad (1)$$

It is determined by the vector potential felt by the electron at the birth time. Equation (2) is valid for laser duration $T \ll \omega_p^{-1}$, where ω_p is the plasma frequency. It is also assumed that the plasma density is sufficiently small so that the effect of plasma dispersion on light propagation can be neglected.

Within the laser pulse, the current increment at time *t* is

$$d\vec{J}_\perp(t) = -e(\vec{p}_\perp(t)/m)dn_e(t) = (e^2/m)W_i(t)n_a(t)\vec{A}_\perp(t)dt, \qquad (2)$$

where, $dn_e(t)/dt = W_i(t)n_a(t)$ is ionisation equation, $W_i(t)$ is tunnelling ionisation rate, and $n_e(t), n_a(t)$ are electron and atom density, respectively. Integrating over the pulse duration $0 \le t \le T$, we obtain the current density at this space point

$$\vec{J}_\perp(\vec{r}) = \frac{e^2}{m}\int_0^T W_i n_a \vec{A}_\perp(t)dt. \qquad (3)$$

Considering an ionized plasma volume with size much smaller than the plasma wavelength $\lambda_p = 2\pi c/\omega_p$, we can integrate the current density $\vec{J}_\perp(\vec{r})$ over the whole plasma volume and obtain the time derivative of the initial dipole for THz emission

* Email: hui-chun.wu@mpq.mpg.de

$$\frac{d\vec{D}_\perp}{dt} = \frac{e^2}{m}\int dr^3 \int_0^T dt W_i n_a \vec{A}_\perp. \quad (4)$$

It builds up in a short time interval $T \ll \omega_p^{-1}$. The dipole $\vec{D}_\perp$ then oscillates and radiates THz waves with the central frequency of $\omega_p / 2\pi$. The emitted THz amplitude has a maximum along the light axis both in forward and backward direction. The peak amplitude is proportional to the dipole amplitude

$$\vec{E}_{THz} \propto d\vec{D}_\perp / dt. \quad (5)$$

It is noted that the 1st peak electric field of THz pulse is proportional to $-d\vec{D}_\perp / dt$.

2. 2DPIC simulation

2.1 2DPIC code

We developed a parallel 2DPIC code. This code employs a simple and fast zigzag scheme [3] for current calculation, and a novel field solver [4], which is free of dispersion in the laser propagation direction. The latter is important for the simulation for the few-cycle pulse case. The ordinary FDTD scheme dramatically changes the CEP of the pulse duo to the numerical dispersion. The second advantage is this scheme does not need the absorption boundary in the laser propagation direction. A plane wave is 100% absorbed at the boundaries. For the tightly focused laser beam, the absorption rate less than 1% can easily be reached. These points are superior to the other schemes and permit the higher-precision simulation.

Our code follows the procedure of Ref. [5] to implement ionisation, using the exact ionisation rates as discussed in Ref. [1]. Here we emphasize that, for the PIC simulation, the light cycle is resolved well, so one should use a *static* tunnelling ionisation rate, which is determined by the instant electron field (not cycle-averaged envelope amplitude).

2.2 Simulation results

Figure 1 shows THz radiation from a H gas target for a linearly polarized laser pulse with the normalized amplitude $a_0 = 0.02$, corresponding to an intensity of $I = 8.6\text{x}10^{14}$ W/cm2. Duration and focal radius of the laser pulse are $T = 4\tau$ (FWHM is 4.1 fs for $\lambda = 800\text{nm}$) and $R = 5\lambda$, respectively, where $\tau = \lambda / c$ is the light cycle. The initial H atom density is $n_0 = 0.0025 n_c$. At the end of the laser pulse, 96:7% of the H atoms close to the light axis are ionised. The radius of the ionised plasma column is $R_p \approx 4.5\lambda$. The plasma length is $L = 10\lambda$. So the deduced plasma size is smaller than $\lambda_p = 20\lambda$. More details about simulation parameters can be found in Ref. [1].

A typical THz pulse is shown in Fig. 1(a) for the CEP $\varphi = 0^\circ$. This THz pulse is effectively single-cycle, and its magnitude approaches 0.12 MV/cm. The circles in Fig. 1(b) give the first peak (also marked in Fig. 1(a) for $\varphi = 0^\circ$) as a function of φ and are compared with model calculation ($-d\vec{D}_\perp / dt.$) from Eq. (4). The dotted curve is obtained when evaluating the volume integral in Eq. (4) for 2D geometry, and the solid curve corresponds to 3D geometry. The difference between the 2D and 3D models lies in the spatial integration of Eq. (4).

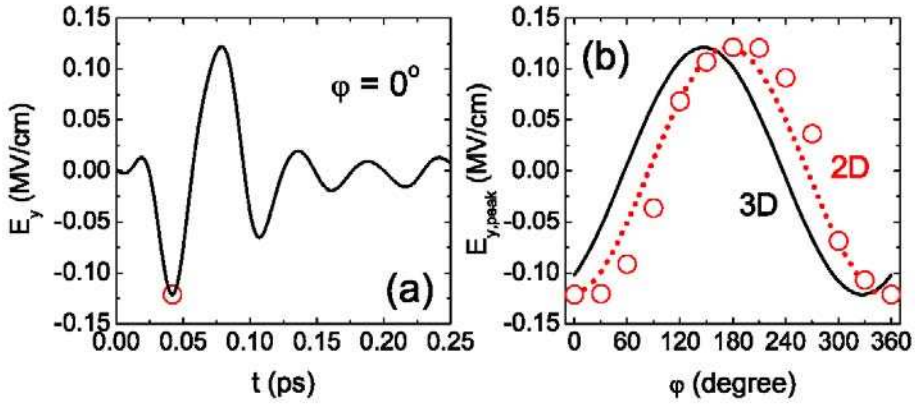

Figure 1. THz emission for the laser pulse with $a_0 = 0.02$. (a) The THz pulse for the phase φ=0°. The circle marks the first peak of this THz pulse. (b) The 1st THz peak as a function of the phase φ. 2D (dotted line) and 3D (solid line) model calculations are based on Eq. (4). The circles are PIC results.

As shown in Fig. 1(b), one finds that the peak amplitude of THz pulses depends on φ sinusoidally. The 2D simulation results naturally agree with the 2D model. There is a phase shift between the 2D and 3D model calculations, which is due to different intensity distributions of 2D and 3D laser beams in the transverse space. The PIC simulation validates the analytical model, so we can use this simple model to exploit the favourable parameters for CEP determination.

3. CEP measurement

By measuring the function $E_{T,peak}(\varphi)$ shown in Figs. 1(b), the absolute phase of the few-cycle pulse can be determined, as it was done in Ref. [6]. This function depends on intensity, duration, and shape of the laser pulse. For determining the CEP, it is necessary to find a region where the function $E_{T,peak}(\varphi)$ is weakly dependent on these laser parameters. Figure 2(a) shows 3D model calculations of $-d\vec{D}_\perp / dt$ for H gas at different laser intensities. We find that $E_{T,peak}(\varphi) \propto -\sin(\varphi + \varphi_0)$, where the offset φ_0 is plotted as a function of laser amplitude a_0 in Fig. 2(b). One observes $E_{T,peak}(\varphi) \propto -\sin(\varphi)$ with offset $\varphi_0 = 0$ for $a_0 \le 0.01$. We find that this constant φ_0 occurs when the final ionisation degree of gas is smaller than 10% (see Fig. 2(a)). As shown in Fig. 2(b), the critical field strength for the constant φ_0 region decreases with the laser duration, since more atoms are ionised for the longer pulse under the same intensity.

To easily understand the distribution $E_{T,peak}(\varphi) \propto -\sin(\varphi)$ with $\varphi_0 = 0$, we show the temporal evolution of laser vector potential and ionised electron density for $\varphi = 0^\circ$ and $\varphi = 90^\circ$ in Figs. 2(c) and 2(d), respectively. Here, the laser pulse has $a_0 = 0.008$ and $T = 4\tau$, and the final ionisation degree of H atoms close to the laser axis is 1.4%. Because ionisation is small, the ionisation peak is the same as for the field peak of the laser pulse and is symmetric around the field peak. For the cosine pulse in Fig. 2(c), one finds that the integration over $dn_e A_\perp$ is exactly zero. For the sine pulse in Fig. 2(d), however, the integration over the two main peaks of ionisation is non-zero and negative. For higher laser intensities, ionisation mainly occurs at an earlier stage of the laser pulse. For example, the

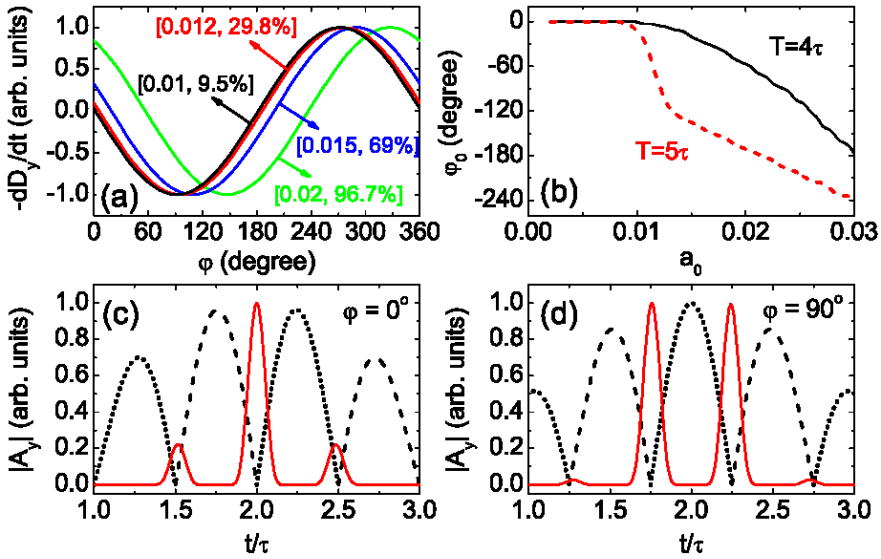

Figure 2. 3D model calculation of THz emission from H gas target. (a) $-dD/dt$ for different laser amplitudes. The brackets give laser amplitude and corresponding final ionization degrees (in percent) of H atoms near the laser axis. The laser pulses have $T = 4\tau$. (b) φ_0 as a function of laser amplitude. Two cases of $T = 4\tau$ and 5τ are plotted. Frames (c) and (d) show the vector potential $|A|$ (dashed lines for positive branches and dotted lines for negative ones) and the instant ionization ratio dn_e/dt (solid lines) for absolute phase (c) $\varphi_0 = 0^o$ and (d) $\varphi_0 = 90^o$.

third ionisation peak in Fig. 2(c) will become weaker and even disappear, which will lead to an effective dipole and causes $E_{T,peak}(\varphi)$ to depart from the distribution of $-\sin(\varphi)$.

4. Conclusions

For CEP measurements, it is best to keep the radiating volume smaller than the plasma wavelength so that the THz radiation emerges essentially from a point dipole. For a typical THz emission with frequency 1 THz (i.e. wavelength 300μm), such configurations can be achieved by using thin gas layers having a thickness of 100μm thick or less. In conclusion, the present paper advances our understanding of photo-ionization induced THz emission in the interaction of few-cycle laser pulses with gases, in particular, when used to determine the absolute phase of the incident pulse. This may help to make this method more accessible for laser control and attosecond experiments.

Acknowledgments
Authors acknowledge support from the Alexander von Humboldt Foundation. HCW is grateful to Prof. Z.-M. Sheng for his encouragements and useful discussions, and appreciate Prof. Sentoku for his generous delivery of the unpublished scheme.

References
[1] Wu H-C, Meyer-ter-Vehn J and Sheng Z-M, New J. Phys. 10, 043001 (2008)
[2] Meyer-ter-Vehn J, Pukhov A and Sheng Z-M Atoms, Solids, and Plasmas in Super-Intense Laser Fields ed Batani D et al. (New York: Kluwer Academic/Plenum) p 167 (2001)
[3] Umeda T, Omura Y, Tominaga T and Matsumoto H, Comput.Phys.Comm. 156, 73(2003)
[4] Sentoku Y 2007 private communication
[5] Kemp A J, Pfund R E W and Meyer-ter-Vehn J, Phys. Plasmas 11, 5648 (2004)
[6] Kreß M *et al.*, Nature Phys. 2, 327 (2006)